Journal of Textiles and Polymers

Vol. 12, No. 1, 36-42, March 2024
https://www.itast.ir
DOI: 10.48302/jtp.2025.544748.1321

The effect of E-glass/carbon hybridization on the buckling behavior of woven fabric reinforced composite laminates

Zinat Sadat Mazloomi, Hadi Dabiryan *

[1] Department of Textile Engineering, Amirkabir University of Technology, Tehran, Iran.

Article Information

Article history:

Received: 2025-09-02

Accepted: 2025-11-01

***Keywords*:**

Buckling, hybrid composites, composite beam theory, carbon and E-glass reinforcements.

Abstract

Hybridization is a technique to enhance the mechanical properties of composites. This paper aims to investigate the effect of hybridization on the buckling behavior of fabric-reinforced composites experimentally, numerically, and theoretically. For this purpose, uniform and hybrid laminates were produced using glass and carbon woven fabrics and epoxy resin. The buckling test was carried out on the prepared samples. The results showed that the hybridization technique enhances the critical buckling loads of laminates. Also, the location of laminas in hybrid laminates significantly affects the buckling behavior of laminates so that the maximum critical buckling load (538.9 kN) belongs to the laminate where the carbon-fabric-reinforced laminas are in outer layers, and the minimum (201.3 kN) belongs to the sample whose outer layers are glass-fabric-reinforced laminas. In addition, a very good correlation was observed between theoretical and numerical results of buckling simulation, which predicted the critical buckling load in FEM based software (ABAQUS).

1 INTRODUCTION

Fabric-reinforced composites are preferred over fiber-reinforced composites to bear buckling loads due to higher resistance to delamination. Composites are commonly used to achieve an economical structure with high mechanical properties, good resistance to chemicals and heat, high physical properties, etc. Nowadays, textile composites are widely used in different industries due to their outstanding properties. Composite laminates are used for bearing different loads and have shown perfect results on the industrial scale [1].

Many investigation methods and computational models have been attempted to understand the compressive, tensile, flexural, and other mechanical behaviors and the damage and fracture mechanics of hybrid composites [2-12].

Different types of hybridization are examined to achieve desirable properties. Ni et al. [13] developed a mathematical formulation to predict the dynamic properties of hybrid beam and plate composites using the finite element energy method. Iyengar and Umeritiya [14] used Kevlar/epoxy and Boron/epoxy hybrid composites and found that these hybrid composites have less weight and tolerate more deflection. Adali and Verijeko [15] designed hybrid laminate plates to achieve the optimum layer arrangement in which the stiffer component is located in outer layers and the softer component is located in inner layers to increase the mechanical properties of the structure. Nayak et al. [16] investigated the buckling behavior of hybrid E-glass and carbon composites with various layer arrangements. They concluded when carbon fiber is increased in composite structures, the critical buckling load is increased too. Ikbal et al. [17,18] produced four-layer interlayer and intralayer hybrid composite laminates by using the unidirectional fabrics of E-glass and carbon, and the tensile and compression tests have been performed for all samples. Murugan et al. [19] fabricated the four-layer hybrid laminate composites using plain-weave E-glass and carbon fabrics as reinforcements with various layer arrangements.

The buckling behavior of laminated composites has been studied by many researchers [16, 20–23]. Amini et al. [20] investigated experimentally the effect of the fabric weave pattern on the buckling behavior of eight-layer fabrics fabricated using plain- and twill-weave E-glass/epoxy laminated composite plates with through-the-width delamination. They observed that the eight-layer plain weave has a greater critical buckling load than the eight-layer twill weave; also, the load-bearing capacity of the eight-layer plain weave is more than the eight-layer twill weave.

Jesri et al. [21] studied analytically the effect of the fabric weave pattern on the buckling behavior of eight-layer plates fabricated using plain-, twill-, and satin-weave E-glass/epoxy laminated composite plates with through-the-width delamination. On the other hand, they used Ishikawa's model

* Corresponding authors: Dabiryan@aut.ac.ir

for simulating the E-glass fabrics as the reinforcement part of laminates. They observed that the load-bearing capacity of the eight layers of satin weave is more than the other eight layers.

Sharif et al. [22] studied the buckling behavior of eight-layer hybrid laminates fabricated using plain- and twill-weave E-glass with various layer arrangements. They observed that the eight-layer twill weave has a greater critical buckling load than the eight-layer plain weave, and also the hybrid samples are stronger than the eight-layer plain-weave samples.

Salehan et al. [23] investigated the buckling behavior of eight-layer fabricated plain-weave E-glass/epoxy laminate composites with high-tenacity polyester yarn through the thickness interlock stitch. They observed that the stitched laminates have a greater critical buckling load than the non-stitched laminates. On the other hand, the elastic properties of samples decreased with the stitch, so the tensile properties of stitched samples are lower than the non-stitched ones.

Previous research has rarely addressed the buckling behavior of hybrid laminated composites analytically. In the present work, we tried to investigate analytically the buckling behavior of glass/carbon hybrid laminated composites. In addition, the effect of hybridization on the buckling behavior of composite laminates is simulated numerically using the ABAQUS/CAE commercial package.

2 MATERIALS AND METHODS

Composite laminas were produced using glass/carbon woven fabrics and epoxy resin as reinforcements and matrix, respectively. The details of fabrics used are presented in Table 1. Also, the mechanical properties of epoxy are shown in Table 2.

Table 1 Technical specification of reinforcement components

Fabric type	Areal density (g/m²)	Warp density (ends/cm)	Weft density (ends/cm)	Thickness (mm)
E-glass	275	8	9	0.25
Carbon T-300	200	6	5	0.27

Table 2 Mechanical and physical properties of matrix components at 23°C

Components	Flexural modulus (GPa)	Flexural strength (MPa)	Tensile modulus (GPa)	Tensile strength (MPa)	Density at 25°C (g/cm³)
Resin Eponate 505	3	126	3.7	73	1.17

The laminas were subjected to the tensile test to obtain the elastic modulus. Fig. 1 shows the stress-strain diagrams of laminas. The elastic modulus was measured as the slope of stress-strain curves. Table III shows the measured elastic modulus of laminas.

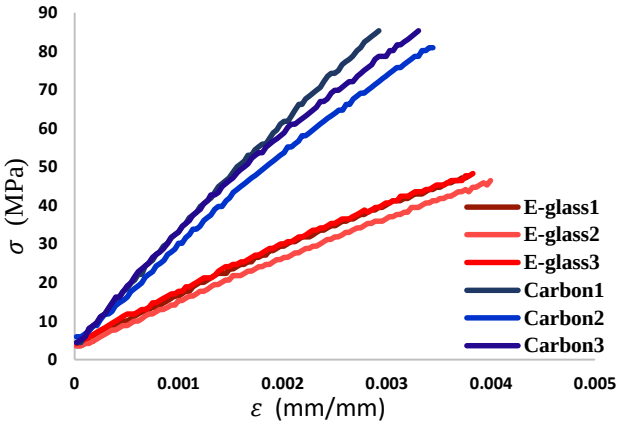

Fig. 1 Stress-strain diagram for single layers of composites

Table 3 The average elasticity modulus of e-glass/epoxy and carbon/epoxy

Single-layer composite	Tag name	Elasticity modulus (GPa)
E-glass/epoxy	E_g	11.4
carbon/epoxy	E_c	25.1

Four-layer hybrid composite laminates were produced using glass- and carbon-reinforced laminas with different layer arrangements by the hand lay-up method. The details of the produced laminates are presented in Table 4.

To calculate the critical buckling load in the experimental test, the buckling test was carried out by exerting the axial compression load using an axial tensile-compression machine having a two-ton load cell. The gripper of the machine is controlled by the pneumatic pressure, which is set at 0.7 MPa. The axial compression force was applied on the sample's cross-section by displacement control technique. For calculating the out-of-plane displacements, two digital gauges were set at the center of the coupon. Fig. 2 shows the buckling test before and after compression load.

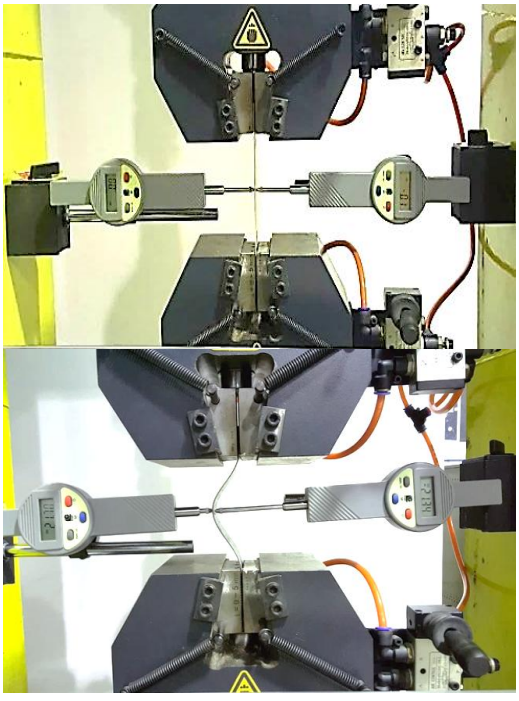

Fig. 2 Buckling test steps, (a) before buckling, (b) after buckling

Table 4 Schematic and details of samples

Sample's Code	Laminate arrangement	Schematic of samples	thickness (mm)	b (mm)	I(mm^4)	radius of gyration (mm)	L(mm)	L/r	volume fraction of fibers (%)	volume fraction of matrix (%)	volume fraction of void (%)
CCCC	(C/C/C/C)		1.16	40	5.21	0.335	100	298.5	54.1	45.9	2.15
EEEE	(E/E/E/E)		1.25	40	6.03	0.352	100	284.2	48.8	51.2	0.87
CEEC	$(C/E)_s$		1.22	40	6.55	0.362	100	276.6	47.6	52.4	1.23
ECCE	$(E/C)_s$		1.09	40	4.31	0.315	100	317.8	51.9	48.0	0.85
CEEE	(C/E/E/E)		1.09	40	4.29	0.314	100	318.3	54.9	45.0	1.13
ECCC	(E/C/C/C)		1.08	40	4.22	0.312	100	320.2	59.7	40.3	2.16

3 THEORETICAL BACKGROUND

One of the popular formulae for calculating critical buckling load is the Euler column formula. The Euler column formula is calculated for the pinned columns. Although the boundary condition of this research is fixed columns, in which the buckling mode for this boundary condition is shown in Fig. 3, the Euler column formula is changed to another form as shown in Eq. (1).

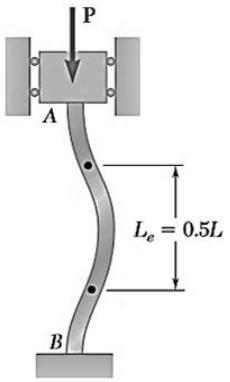

Fig. 3 Buckling mode for fixed column [24]

Based on the Euler column formula for clamped-clamped support:

$$P_{cr} = \frac{4\pi EI}{L_e^2} \quad (1)$$

Where E is the elasticity modulus, I is the second moment of area, and L_e is the effective length of the column as shown in Fig. 1.

Based on the theory of composite beams, the flexural rigidity (B) of the hybrid laminates is obtained in Eq. (2):

$$B = (E\,I)_{eq} \quad (2)$$

Where, $(E\,I)_{eq} = E_1 I_1 + E_2 I_2$

The E_1 and E_2 are the elastic modulus, and I_1 and I_2 are the moments of inertia of beams 1 and 2, respectively, and $(E\,I)_{eq}$ is the equivalence of the flexural rigidity. Eight types of four-layer laminates, including uniform and hybrid laminates, are considered for this research. Considering the theory of composite beam, for instance, the flexural rigidity of CEEC can be defined as below:

The first step is to convert the carbon layer to the E-glass layer with respect to the ratio of modulus, which is obtained as below:

$$n = \frac{E_c}{E_g}$$

The second step is locating the neutral axis for the transformed section, as shown in Fig. 4.

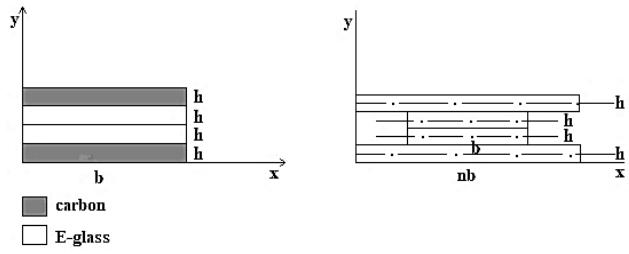

Fig. 4 Schematic of a four-layered hybrid composite transformed of CEEC

The details of the second moment of area for each layer are shown in Table 5.

$$I_g = moment\ of\ inertia\ of\ each\ layer + Ad^2 \quad (3)$$

Table 5 Necessary parameters for calculating the I_g

Layer No.	I_0	A	d^2	Ad^2	I_0+Ad^2
1	$\frac{nbh^3}{12}$	nbh	$(2h-\frac{1}{2}h)^2$	$\frac{9}{4}nbh^3$	$\frac{nbh^3}{12}+\frac{9}{4}nbh^3$
2	$\frac{bh^3}{12}$	bh	$(2h-\frac{3}{2}h)^2$	$\frac{1}{4}bh^3$	$\frac{bh^3}{12}+\frac{1}{4}bh^3$
3	$\frac{bh^3}{12}$	bh	$(2h-\frac{5}{2}h)^2$	$\frac{1}{4}bh^3$	$\frac{bh^3}{12}+\frac{1}{4}bh^3$
4	$\frac{nbh^3}{12}$	nbh	$(2h-\frac{7}{2}h)^2$	$\frac{9}{4}nbh^3$	$\frac{nbh^3}{12}+\frac{9}{4}nbh^3$

The moment of inertia of laminates is obtained by adding the moment of area of laminas as follows in Eq. (4):

$$I_g = \frac{bh^3}{12}(56n+8) \quad (4)$$

By substituting Eq. (4) into Eq. (2), the resultant elasticity modulus of the CEEC laminate will be Eq. (5):

$$E_r = \frac{7E_c + E_g}{8} \quad (5)$$

Table 6 The resultant elasticity modulus for hybrid composite samples

Layer arrangement	$\bar{Y}_0$	I_g	E_r
CEEC	$2h$	$\frac{bh^3}{12}(56n+8)$	$\frac{7E_c+E_g}{8}$
ECCE	$2h$	$\frac{bh^3}{12}(8n+56)$	$\frac{7E_g+E_c}{8}$
CEEE	$\frac{(15+n)}{(2n+6)}h$	$(n+3)\frac{bh^3}{12}+bh^3\frac{2(7n+3)}{(n+3)}$	$\frac{E_c^2+174E_cE_g+81E_g^2}{64(E_c+3E_g)}$
ECCC	$\frac{(15n+1)}{(6n+2)}h$	$(3n+1)\frac{bh^3}{12}+bh^3\frac{2n(3n+7)}{(3n+1)}$	$\frac{81E_c^2+174E_cE_g+E_g^2}{64(3E_c+E_g)}$

Using derived formulas for the elastic modulus of the laminate shown in Table VI and Eq. (1), the critical buckling loads of laminates were calculated. The elastic modulus of glass and carbon layers is 11.8 and 25.1 GPa, respectively. Therefore, the parameter 'n' is equal to 2.2 for all samples. The samples have a width of 40mm and a length of 100mm. The values of theoretical buckling loads are presented in Table 7.

The comparison between the experimental and theoretical critical buckling loads has been presented in Table 8. As shown, except for the EEEE sample, a reasonable error percentage in the prediction of critical buckling load has been recorded.

Table 7 The critical buckling load by using the analytical method

Layer arrangement	Thickness (mm)	I (mm^4)	E_r (MPa)	P_{cr} (N)
CCCC	1.161	5.212	25125	516
EEEE	1.219	6.035	11354	270
CEEC	1.253	6.55	23404	605
ECCE	1.09	4.317	13075	223
CEEE	1.088	4.296	16028	272
ECCC	1.082	4.221	18178	303

Table 8 Comparison between experimental and theoretical results

Sample's Code	P_{cr} (N)		Error (%)
	Theory	Experimental	
CCCC	516	426	17.4
EEEE	270	176	34.8
CEEC	605	539	10.9
ECCE	223	202	9.4
CEEE	272	236	13.2
ECCC	303	271	10.5

4 RESULTS AND DISCUSSIONS

The Southwell method was applied to obtain the critical buckling load. In this method, the critical buckling load is measured as the slope of the diagram of lateral displacement (W) versus the ratio of the lateral displacement to the applied pressure load (W/P). The Southwell diagram was plotted before the post-buckling region. Southwell plots of different samples are drawn in Fig. 5.

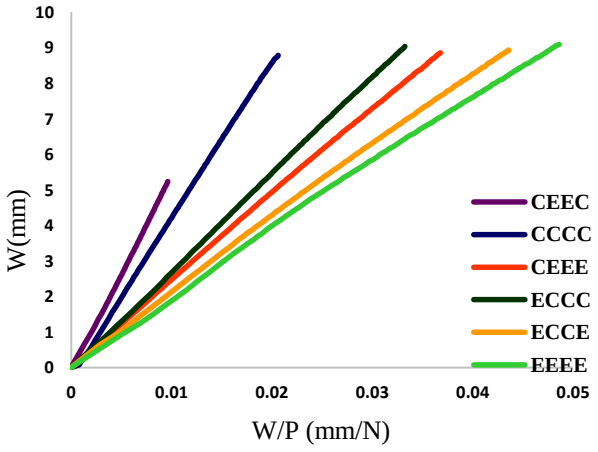

Fig. 5 Southwell plots for different samples

The critical loads obtained from the Southwell method are presented in Table 9. The results are discussed in two categories: uniform laminates and hybrid laminates. As results show, in the uniform laminates, the critical buckling load of the CCCC laminate is greater than that of the EEEE laminate, which is attributed to the higher modulus of carbon fabric reinforced laminas in comparison with glass fabric reinforced laminas.

Table 9 The average critical buckling load based on the Southwell method

	Sample's Code	P_{cr} (N)
Uniform laminates	CCCC	426.06
	EEEE	175.59
Hybrid laminates	CEEC	538.9
	ECCE	201.34
	CEEE	236.01
	ECCC	271.05

In hybrid laminates, the maximum critical buckling load (538.9 kN) belongs to the CEEC, where the carbon-fabric-reinforced laminas are in outer layers, and the minimum (201.3 kN) belongs to the ECCE, whose outer layers are glass-fabric-reinforced laminas. As indicated, the location of laminas significantly affects the buckling behavior of laminates. It is worth noting that, although the ECCC sample has a higher number of stiff layers than the CEEC sample, its critical buckling load is less than that of the CEEC sample. By comparing the maximum critical buckling loads of uniform and hybrid laminates, it can be seen that the hybrid laminates tolerate more critical buckling loads.

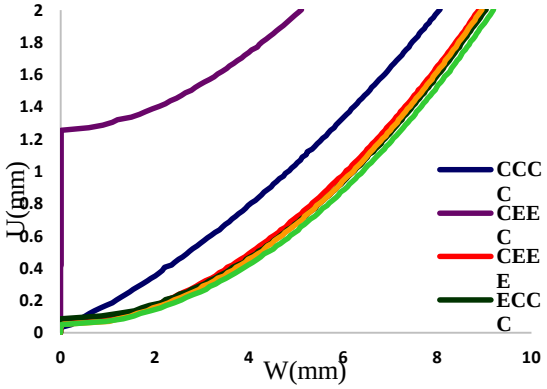

Fig. 6 End-shortening (U) vs. lateral displacement (W)

Based on the graphs of Fig. 6, the CEEC sample has the most stability among all laminates. In other words, the CEEC sample has the most critical buckling load and the most stability among all samples.

5 NUMERICAL SIMULATION

In the present work, eigenbuckling analysis was performed to simulate the buckling behavior of composite laminate beams. The element type of C3D20R was chosen to create the mesh for laminated composite beams as shown in Fig. 7. The following boundary conditions were set to the clamped end:

Top side $\begin{cases} u_1 = 0;\ u_2 \neq 0;\ u_3 = 0 \\ UR_1 = 0;\ UR_2 = 0;\ UR_3 = 0 \end{cases}$

Bottom side $\begin{cases} u_1 = 0;\ u_2 = 0;\ u_3 = 0 \\ UR_1 = 0;\ UR_2 = 0;\ UR_3 = 0 \end{cases}$

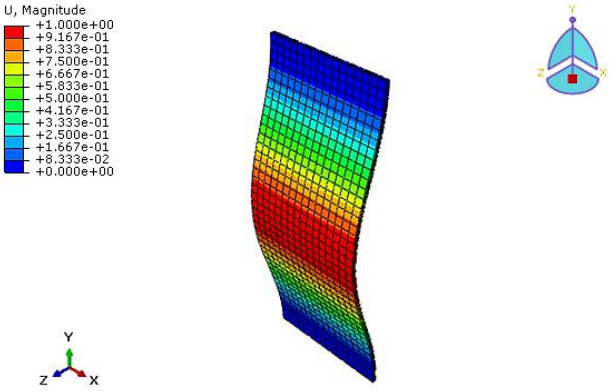

Fig. 7 Schematic of samples in ABAQUS software

For the accuracy of the simulation, a path through the center of the sample is chosen, and Fig. 8 reports the buckling mode of fixed columns just as noted before.

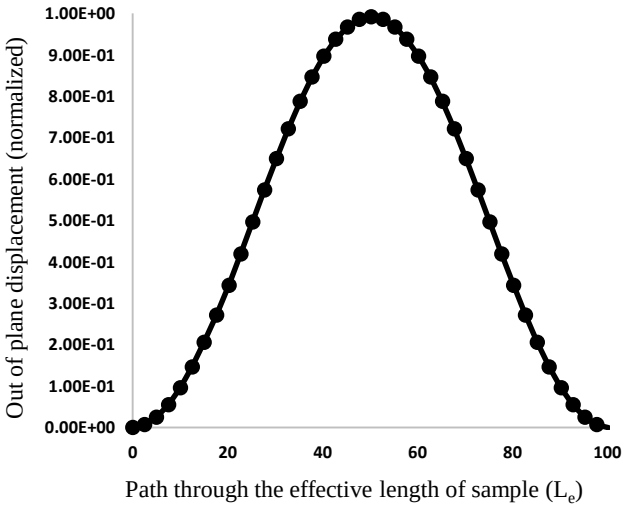

Fig. 8 Buckling mode created in ABAQUS software for the fixed column

A comparison between the experimental critical buckling load and the numerical critical buckling load is reported in Table 10.

Table 10 Comparison between experimental and numerical results

Sample's Code	P_{cr} (N)		Error (%)
	Num.	Exp.	
CCCC	517	426	17.6
EEEE	272	176	35.3
CEEC	605	539	10.9
ECCE	224	202	9.8
CEEE	272	236	13.2
ECCC	303	271	10.5

Fig. 9 shows the results of the numerical, experimental, and theoretical results of critical buckling loads as bar charts. As can be seen, there is a very good correlation between theoretical and numerical results that confirms the accuracy of the performed simulation. Also, the bar charts reveal that all experimental results are less than both the numerical and theoretical results. This is attributed to some imperfections in the actual condition of the buckling test.

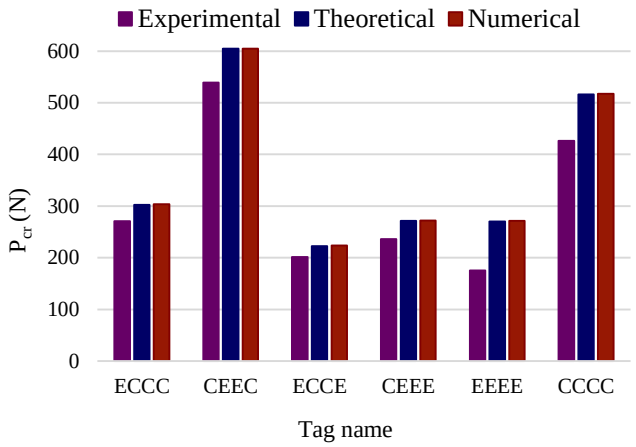

Fig. 9 Comparison of experimental, theoretical, and numerical critical buckling loads

6 CONCLUSIONS

The buckling behavior of uniform and hybrid E-glass/carbon laminates was studied numerically, theoretically, and experimentally. The following results were obtained:

- The hybridization technique improves the buckling behavior of composite laminates.
- In hybrid laminates, the location of laminas significantly affects the buckling behavior of the laminates.
- The maximum critical buckling load is 538.9 kN and belongs to the laminate where the carbon-fabric-reinforced laminas are in outer layers, and the minimum critical buckling load is 201.3 kN and belongs to the sample whose outer layers are glass-fabric-reinforced laminas.
- A very good agreement was observed between the theoretical and numerical results of the buckling simulation.
- The maximum error in predicting the critical buckling load of hybrid laminates is about 13.5%, which is a reasonable error of prediction for fabric-reinforced composites.

REFERENCES

[1] Kaw, A.K., 2005. Mechanics of composite materials, (Vol. 29). CRC Press.

[2] Naik, N.K. and Kumar, R.S., 1999. Compressive strength of unidirectional composites: evaluation and comparison of prediction models. Composite Structures, 46(3), pp.299–308.

[3] Dong, C. and Davies, I.J., 2014. Flexural and tensile moduli of unidirectional hybrid epoxy composites reinforced by S-2 glass and T700S carbon fibers. Materials & Design, vol. 54, pp.893–899.

[4] Manders, P.W. and Bader, M.G., 1981. The strength of hybrid Glass/Carbon fiber composites. I: Failure strain enhancement and failure mode. Journal of Materials Science, 16(8), pp.2233-2245.

[5] Davies, I.J., 2008. Flexural failure of unidirectional hybrid fiber-reinforced polymer (FRP) composites containing different grades of glass fiber. Advanced Materials Research, 41, pp.357–362.

[6] Summerscales, J. and Short, D., 1978. Carbon fibre and glass fibre hybrid reinforced plastics. Composites, 9(3), pp.157–166.

[7] Piggott, M.R. and Harris, B., 1981. Compression strength of hybrid fiber-reinforced plastics. Journal of Materials Science, 16(3), pp.687–693.

[8] Lark, R.F. and Chamis, C.C., 1986. Fabrication and quality assurance processes for super hybrid composite fan blades. Composites Technology and Research, 8(3), pp.98–102.

[9] Banerjee, S. and Sankar, B.V., 2014. Mechanical properties of hybrid composites using finite element method based micromechanics. Composites Part B: Engineering, 58, pp.318–327.

[10] Bazhenov, S.L., Kuperman, A.M., Zelenskii, E.S. and Berlin, A.A., 1992. Compression failure of unidirectional glass-fiber-reinforced plastics. Composites Science and Technology, 45(3), pp.201–208.

[11] Budiansky, B. and Fleck, N.A., 1993. Compressive Failure of fibre composites. Journal of Mechanics and Physics of Solids, 41(1), pp.183–211.

[12] Bunsell, A.R. and Harris, B., 1974. Hybrid carbon and glass fibre composites. Composites, 5(4), pp.157–164.

[13] Ni, R.G., Lin, D.X. and Adams, R.D., 1984. The dynamic properties of carbon-glass fiber sandwich-laminated composites: theoretical, experimental and economic considerations. Composites, 15(4), pp.297–304.

[14] Iyengar, N.G.R. and Umaretiya, J.R., 1986. Deflection analysis of hybrid laminated composite plates. Composite Structures, 5(1), pp.15–32.

[15] Adali, S. and Verijenko, V.E., 2001. Optimum stacking sequence design of symmetric hybrid laminates undergoing free vibrations. Composite Structures, 54(2–3), pp.131–138.

[16] N. Nayak, , S. Meher, , and S.K. Sahu, "Experimental and numerical study on vibration and buckling characteristics of glass-carbon/epoxy hybrid composite plates", In: Proceedings of International Conference on Advances in Civil Engineering, AETACE; pp 888–895, 2013.

[17] Ikbal, H., Wang, Q., Azzam, A., and Li, W., 2016. Effect of hybrid ratio and laminate geometry on compressive properties of carbon/glass hybrid composites. Fibers and Polymers, 17(1), pp.117–129.

[18] Ikbal, M.H., Ahmed, A., Qingtao, W., Shuai, Z. and et al., 2017. Hybrid composites made of unidirectional T600S carbon and E-glass fabrics under quasi-static loading. Journal of Industrial Textiles, 46(7), pp.1511–1535.

[19] Murugan, R., Narasimhan, R.L., and Harish, A., "Effect of Fiber Orientation on Effective Stacking Sequence of Glass/Carbon Hybrid Composite Laminates for Structural Applications", In: International Conference for Phoenixes on Emerging Current Trends in Engineering and Management (PECTEAM 2018); pp. 204–210, 2018.

[20] Amini, E., Jeddi, A.A.A., Ovesy, H.R., and Dabiryan, H., "Influence of fabric weave pattern on buckling behavior of fabric reinforced composite plates with through the width delamination", In: 16th Europen Conference Composites Materials ECCM 2014; pp. 22–26, 2014.

[21] Dabiryan, H., Jesri, M., Ovesy, H.R. and Mazloomi, Z.S., 2022. Numerical and experimental study of buckling behavior of delaminated plate in glass woven fabric composite laminates. Journal of Engineered Fibers and Fabrics, 17, p.15589250221091268.

[22] Dabiryan, H., Mazloomi, Z.S. and Sharif-Deljuee, O., 2024. Effect of fiber path on the buckling behavior of delaminated composites reinforced with woven fabrics; analytical and numerical study. Fibers and Polymers, 25(3), pp.1047-1059.

[23] Salehan, H., Oveysi, H., and Dabiryan, H., "Buckling Enhancement of E-Glass/Epoxy Composite Laminates by Through-the-thickness Stitches", In: The Biennial International Conference on Experimental Solid Mechanics (X-Mech 2020), Tehran, Iran, 2020.

[24] Beer, F.P., Jr., E.R.J., Dewolf, J.T., and Mazurek, D.F., 2015. Mechanics of materials, McGraw-Hill Education, 7th ed., , pp. 698-702.